

# INITIAL INVESTIGATION OF A LOW-COST AUTOMOTIVE LIDAR SYSTEM

A. Ortiz Arteaga, D. Scott, J. Boehm\*

Dept. of Civil, Environmental & Geomatic Engineering, University College London, Gower Street, London, WC1E 6BT UK  
angelica.arteaga.17@ucl.ac.uk, d.scott@ucl.ac.uk, j.boehm@ucl.ac.uk

## Commission II

**KEY WORDS:** LIDAR, Low-Cost, Automotive

### ABSTRACT:

This investigation focuses on the performance assessment of a low-cost automotive LIDAR, the Livox Mid-40 series. The work aims to examine the qualities of the sensor in terms of ranging, repeatability and accuracy. Towards these aims a series of experiments were carried out based on previous research of low-cost sensor accuracy, LIDAR accuracy investigation and TLS calibration experiments. The Livox Mid-40 series offers the advantage of a long-range detection beyond 200 m at a remarkably low cost. The preliminary results of the tests for this sensor indicate that it can be used for reality capture purposes such as to obtain coarse as-built plans and volume calculations to mention a few. Close-range experiments were conducted in an indoor laboratory setting. Long-range experiments were performed outdoors towards a building façade. Reference values in both setups were provided with a Leica RTC 360 terrestrial LIDAR system. In the close-range experiments a cross section of the point cloud shows a significant level of noise in the acquired data. At a stand-off distance of 5 m the length measurement tests reveal deviations of up to 11 mm to the reference values. Range measurement was tested up to 130 meters and shows ranging deviations of up to 25 millimetres. The authors recommend further investigation of the issues in radiometric behaviour and material reflectivity. Also, more knowledge about the internal components is needed to understand the causes of the concentric ripple effect observed at close ranges. Another aspect that should be considered is the use of targets and their design as the non-standard scan pattern prevents automated detection with standard commercial software.

## 1. INTRODUCTION

### 1.1 General Introduction

Laser scanning has become a very commonly used method for reality capture, gaining popularity in many fields such as the architecture, engineering and construction (AEC) sector. A primary reason for this technique's popularity is due to its many applications. Some of these applications include deformation monitoring, High Definition Surveying (HDS), 3-Dimensional (3D) modelling and capturing data for the Building Information Modelling (BIM) process (Thomson and Boehm, 2014). Moreover, Reality Capture (RC), has become a vital asset for collecting data in new industries. Examples of these comprehend autonomous vehicles, virtual and augmented reality amongst others. The incorporation of this technology is due to an ever-growing demand for agents to be aware and understand their surroundings. Even for industries that do not collect data on first-hand but rely on extensive public/private datasets, i.e. environmental monitoring.

In recent years considerable efforts have been spent for creating the autonomous car of the future. Many interested parties see state-of-the-art LIDAR technology as a key technology for the automotive industry. Several established companies and a multitude of start-up companies have developed and adopted LIDAR technology into vehicles for navigation. Autonomous vehicles could navigate in constrained environments surrounded by mobile objects hence, they have to continuously observe the drivable space to enrich passengers and third person safety (Moras et al., 2012).

Although this new generation of low-cost, small LIDAR sensors may not have the same standards as established surveying

equipment, they should not be overlooked, as they could still provide interesting solutions for the AEC industries.

In the United Kingdom, the Royal Institution of Chartered Surveyors (RICS) recommendations for professional surveying tasks state that not all projects require the same level of accuracy (Royal Institution of Chartered Surveyors, 2014). This means that different methods and devices can be utilised for a job. Therefore, not all tasks require the same amount of resources. Typically, the cost of a LIDAR or Terrestrial Laser Scanner (TLS) is influenced by the accuracy that it can deliver. The rise of novel low-cost scanner extends the options of tools that can be used for RC, unveiling a niche in the market for the RC and AEC industries and creating the possibility of increasing direct costumers' profitability and deliver a custom-tailored service to end-users of LIDAR-derived products.

Besides the cost of an instrument and its accuracy requirements, the resolution of a LIDAR is another matter of importance, as this aspect affects the level of details that can be observed from a point cloud. As a consequence, this condition has a direct implication on the quality of the 3D model that could be obtained (Ling et al., 2008). Additionally, previous research of low-cost 3D sensors mentions that accuracy and repeatability are crucial when assessing structured- light-based 3D sensors (Boehm, 2014).

### 1.2 Introduction to the Livox Mid-40 series

In this study we want to investigate the capabilities of a new automotive LIDAR system that became available to the market in 2019 for only \$600. This is significantly below the cost of establishes automotive LIDAR systems which often have a price that is an order of magnitude higher. The Livox Mid-40 series

\* Corresponding author



Figure 1. Livox Mid-40 LIDAR sensor

Laser Wavelength	905 nm
Detection Range	90 m @ 10% reflectivity 130 m @ 20% reflectivity 260 m @ 80% reflectivity
Field of view	38.4° circular
Range Precision	0.02 m
Angular accuracy	< 0.1°
Beam divergence	0.28° (vert.) x 0.03° (horiz.)
Dimension	88 x 69 x 76 mm
Weight	760 g
Price	600 US\$

Table 1: Specifications of the Livox MID-40 as given by the manufacturer

LIDAR is an instrument that was developed by Livox Technology primarily for the automotive market. Table 1 contains a few basic specifications of the sensor as provided by the manufacturer (Livox, 2019a).

The manufacturer user manual states a detection range of up to 260 metres, with some limitations on reflectivity. This puts the sensor firmly in competition with more established terrestrial LIDAR sensors and separates it from typical consumer grade 3D sensors. The manual mentions several possible application scenarios applications: “autonomous driving, robot navigation, dynamic path planning and high-precision mapping”. The sensor’s field of view is a cone with an opening angle of 38 degrees. This is reminiscent of very early terrestrial LIDAR sensors in the surveying market, often referred to as ‘window-scanners’.

Unfortunately, little is known at the time of writing about the unit’s scanning mechanism. The manufacturer’s web page specifically states that the sensor units do not “contain any moving electronic components” (Livox Technology, 2019). However, this is not the same as claiming it to be a solid-state LIDAR. The unit’s principle is described as a non-repetitive scanning technology, where point density increases over time. The scan pattern is fixed and cannot be changed by the user.

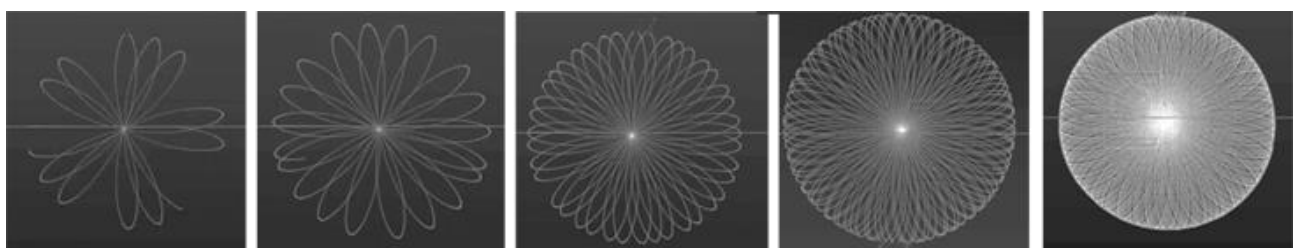


Figure 2. The sensor’s scan pattern with the point cloud becoming denser over time.

Figure 2 exposes the scan pattern, by displaying the point cloud integrated at different points in time. This scan pattern is not consistent with a dual-axis gimbaled mirror scanner. For this we would expect a Lissajous pattern. The graphs do however resemble a rosette shaped pattern created by a Risley prism scanner (THORLABS, 2019). A Risley scanner consists of two wedge prisms that rotate around a common axis (Marshall, 1999). Depending on the ratio of the rotation speeds of the two prisms several patterns can be created which are either stable repetitive curves or non-repetitive space filling curves. It must be stated that this could only be assumed as the manufacturer does not provide detailed information about the technology that was used in the design of the scanner.

The sensor unit comes with a control software, specially designed for Livox LIDAR sensors. This software is used to record and display the real-time data within the FOV. The obtained 3D data can be exported to LAS format (“LAS Specification Version 1.3,” 2009). The Livox Viewer 0.5.0 (Livox, 2019b) as well as a Software Developer Kit (SDK) are available directly from the manufacturer.

The Livox Mid-40 series specifications were used to inform the design of the experiments described in this investigation. These values were considered for the test set-up, especially the possible ranges, precision and angular accuracy. Verifying these values was the main aim of this investigation. Establishing these characteristics helps to build a complete picture of the instrument’s behaviour as well as the limitations that the instrument could encounter in applications. Typically, specification values are obtained in controlled environments, which are difficult to recreate in a real-world situation. We attempted to repeat every measurement several times to gain better understanding of the repeatability of performance characteristics. However, not all characteristics that are relevant for a sensors suitability could be established in a quantitative manner. In part this is due to the lack of standards, but in part also due to some surprising behaviour the sensor has exhibited. We therefore split the experimental section into two, one for qualitative observations and one for quantitative assessment.

## 2. QUALITATIVE OBSERVATIONS

To have a first impressions of the sensor’s performance, some simple tests were performed. The aim was to capture point clouds of some typical objects and visually inspect the 3D data. Tests were performed for the long and short-range in an indoor and outdoor setting respectively. These tests comprised the behaviour of the instrument *per se* and the quality of the data that could be obtained from the scanner for the long and short-range as for an indoors and outdoors operation.

### 2.1 Scan Pattern

It was confirmed that the coverage of the FOV improves with time. The short-range tests show visually that the density and

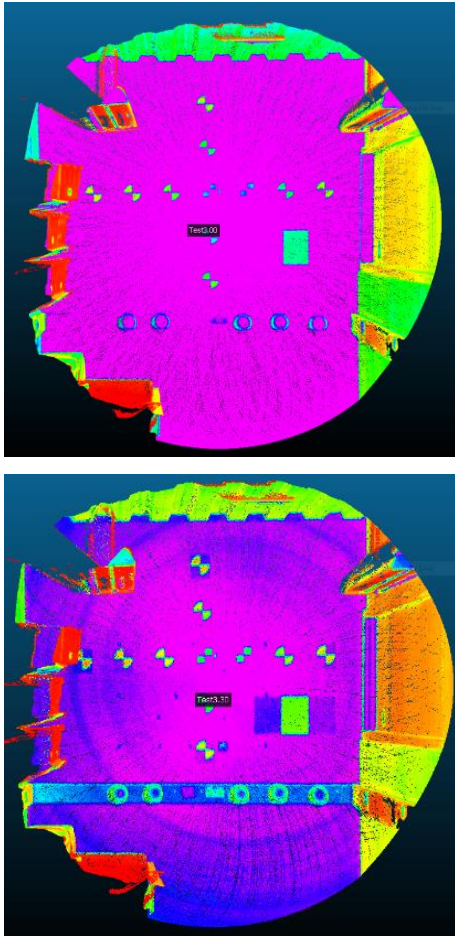


Figure 3. Point cloud captured at short-range. Data is integrated for less than minute (top) and 30 minutes (bottom).

detail of the point cloud increases with longer integration times. After 15 minutes of continuous scanning more details could be observed from the point cloud. It was only after 30 minutes of uninterrupted data collection that most details present on the test scenario were also visible on the point cloud. Figure 3 compare the detail obtained with an integration time of less than 1 minute and an integration time of 30 minutes.

This sensor does not collect points in a grid-like pattern as would be expected from typical terrestrial laser scanning systems. The rosette-like pattern causes some variations in the definition and resolution across the field of view. As the point density is not constant it is difficult to precisely identify or measure objects at a constant accuracy. This is particularly problematic for

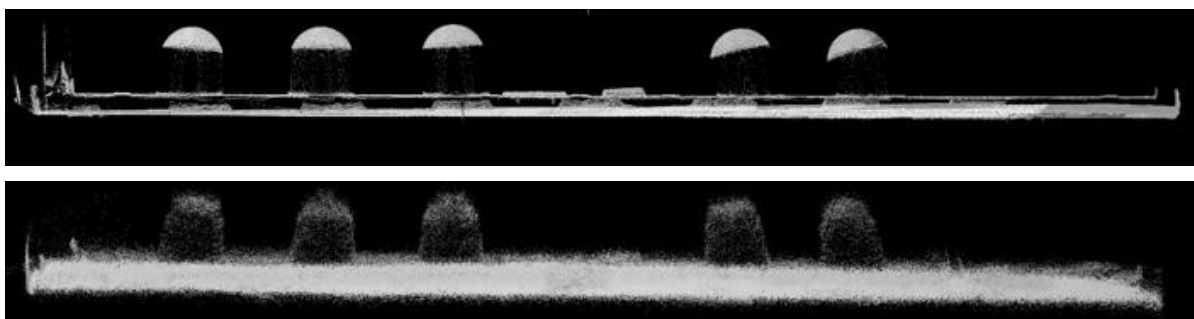


Figure 4. Comparison of point clouds over several sphere targets. Top shows Leica RTC360, bottom row shows Livox MID-40.

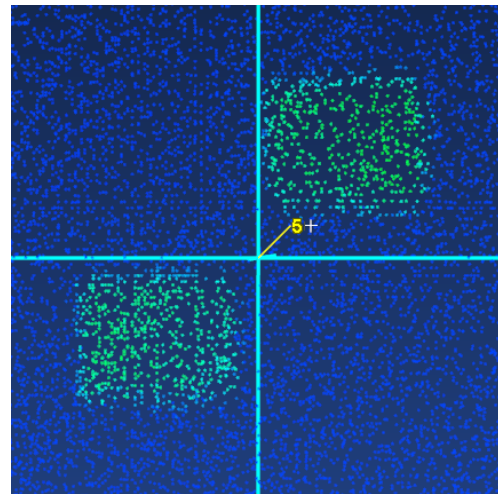


Figure 5. Centre of checker-board target with a visible gap in-between the two black squares.

measuring artificial targets which are often used in terrestrial surveying. We show two types of targets commonly used in lasers scanning: checker-board targets and spheres.

Figure 5 shows the point cloud over a standard checker-board target. It was not possible to automatically measure the target centre using available commercial software. We believe that this is in part due to the atypical scan pattern. We also observe an unusual gap in-between the two black squares that make up the pattern. Ideally, they should meet in the centre point. This leaves an additional uncertainty in manually measuring the target's centre point.

Likewise, standard commercial software was also unable to automatically identify and measure sphere targets from the sensor's point cloud. Figure 4 shows the point cloud obtained with the Livox MID-40 compared to a reference instrument the Leica RTC360. The level of noise is clearly visible as well as the 'ghost' points commonly created by mixed pixel effects.

## 2.2 Point Density

From the early experiments we settled to capture single scans with integration times of 5 seconds. This generates point clouds of about 300,000 points. Multiple of these single scans then can be added to create denser point clouds. In this way we create a point cloud of approximately 1,800,000 points of a facade at long range. Figure 6 shows the variation of the point density computed using Cloud Compare (Girardeau-Montaut, 2011). It is clearly visible that the density is the highest at the centre of the scan

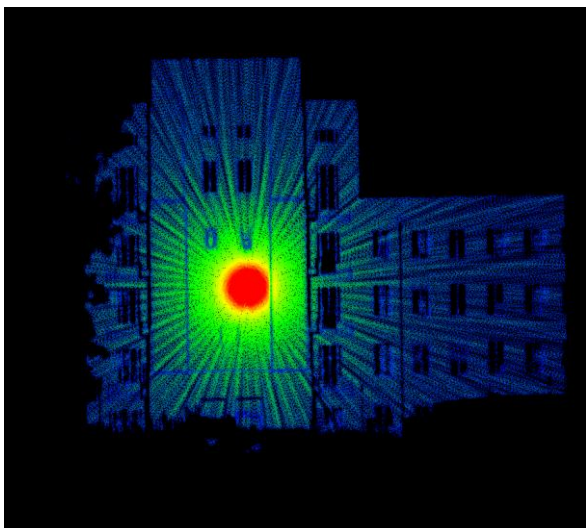


Figure 6. Point cloud density

pattern. We can also observe a star-shaped pattern as density decreases away from the centre.

### 2.3 Ripple Effect

Every point cloud that was obtained with the Livox MID-40 in indoors tests contains some noise artefacts which propagate along the point cloud, similar to water ripples. This effect obviously has influence on range and angular measurements. It is best visible when observing a planar object. Figure 7 shows the effect on a scan of a wall. This effect could be attributed to the potential use of a Risley prism or potential fluctuation on the laser's frequency. But not enough is known about the hardware's details to make that assessment.

### 2.4 Radiometric Influences

Another observation relates to the laser wavelength and the reflectivity on different colour or material. The Livox MID-40 is

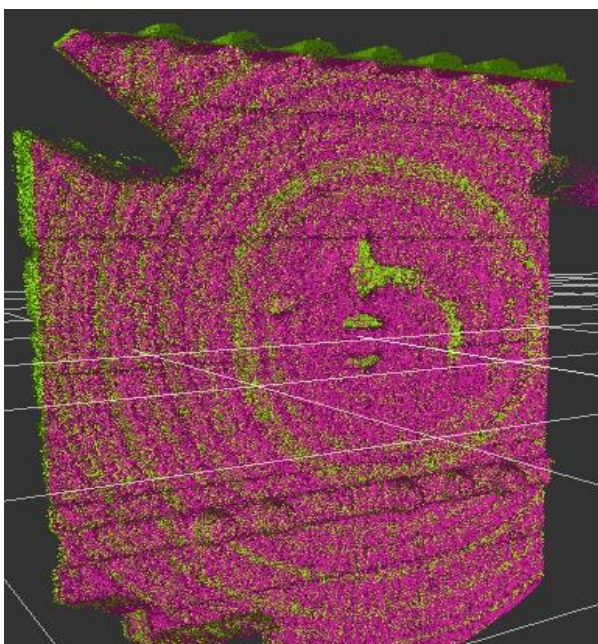


Figure 7. Ripple effect on point cloud

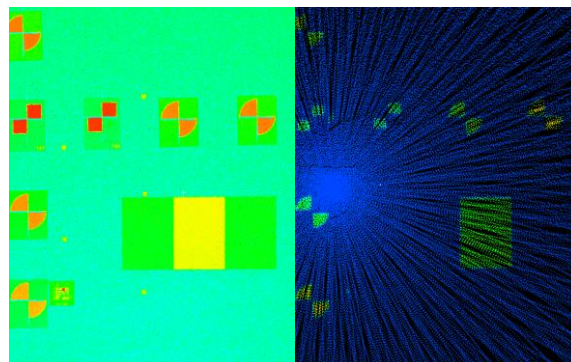


Figure 8. Leica RTC360 (left) and Livox MID-40 (right) point on different material.

specified to use a 905 nm source. Figure 8 shows a scan of three printed sheets of paper with different grey values at the centre (see also Figure 10). The point cloud shows reflected intensity as false colour for better visibility. The MID-40 cannot distinguish the brightest and the darkest pattern from the background of a white wall. However, our reference instrument the Leica RTC360, which operates at 1550 nm, can clearly separate them from the background. It is curious that after longer integration times the radiometric resolution of the instruments seems to improve (compare Figure 3).

We can observe that for the Livox MID-40 the reflected intensity has a direct influence on the range measurements. This is shown in Figure 9. While the object is a planar target, the point cloud shows a difference in depth depending on the intensity. Lighter colours are detected as 'nearer' while darker colours seem to be further away. While this effect and its causes are generally known, they have long since been eliminated in most survey-grade instruments.

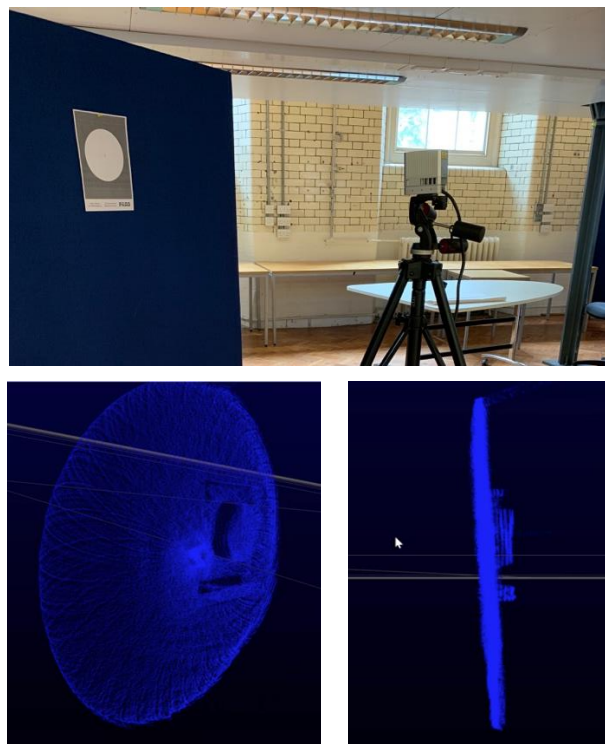


Figure 9. Scanning a planar circular target printed on paper.

### 3. QUANTITATIVE TEST

Given the lack of specific guidelines for verifying 3D sensors in large volumes we adapt the existing guidelines for optical 3D sensors in small volumes. Particularly we are aligning our tests to the VDI 2634 Part 2 guidelines (“VDI-Richtlinie: VDI/VDE 2634 Blatt 2 - Optische 3D-Messsysteme - Bildgebende Systeme mit flächenhafter Antastung,” 2002). We have successfully relied on this guideline in previous works on sensor tests (Boehm, 2014) and its terminology is widely accepted in both the scientific community and in industry. We then conducted experiments in length measurements over a smaller indoor test field of approximately 2 meters by 1.5 meters from a distance of about 5 meters. We conducted experiments in ranging accuracy outdoors towards a flat façade at ranges from 40 to 130 meters. In the same test setup, we have also tested for planarity.

#### 3.1 Length Measurement

The test field consists of 11 checkerboard targets arranged in the shape of a cross as shown in Figure 10. The spacing of the targets is about 30 centimetres. This arrangement allows to check 21 lengths in the horizontal direction from 0.3 meters to 2 meters and 10 lengths from 0.3 meters to 1.5 meters in the vertical direction. We repeat the experiments seven times at different times in 5-minute intervals. This is to ensure we have no thermal effects from the sensor unit heating up, which might affect performance.



Figure 10: Test sites for the length measurement (top) and range measurement (bottom) test.

We gather reference values for the lengths with a reference instrument a Leica RTC 360 terrestrial laser scanner. From previous experience we expect the instrument to detect target centres to an accuracy of a millimetre. The deviations of the length measurements between the two instruments are plotted as a graph over the increasing length as suggested in VDI 2634. We separate plot from horizontal deviations from vertical deviations. This is to uncover any bias in the scanning mechanism. For brevity we only show 3 of the 7 experiments at 0, 5 and 30 minutes in Figure 11.

The deviations typically stay with a span of 10 millimetres and seem randomly distributed. The analysis shows no effect of the absolute length measured to the deviation from reference. This is as expected for a time-of-flight system. There is no discrepancy in horizontal deviations compared to vertical deviations. This would be in line with the assumed rotating scanning mechanism. The sensor’s length measurement behaviour does not change over the observed time interval of ½ hour. This cannot always be expected for a low-cost system.

All length captured in this test are on a plane perpendicular to the sensor’s optical axis. VDI 2634 would have recommended a spatial distribution of the lengths across a define measurement volume. We can use this simplified test to get an indication of the accuracy in the sensor’s directional measurement. With a trigonometric approximation, neglecting any errors in ranging, we can estimate the angular accuracy from the deviation in length. With respect to the optical axis 1 mm in length measurement error corresponds to 1 hundredth of a degree in angular measurement. Likewise, 10 millimetres correspond to 1 tenth of a degree.

#### 3.2 Range Measurement

We have conducted outdoor ranging experiments to test the sensor over longer ranges. As the laser beam is continuously spinning and its direction cannot be directly controlled it is difficult to directly assess the ranging quality. We thus try to approximate that test by assessing the ranging behaviour onto a planar object. We observe a planar sand-stone facade from distances at 40, 60, 90 and 130 meters away (see Figure 10). We fit a plane to the point cloud of the façade and calculate the distance of the sensor to the plane. The calculated range is thus not a single point range measurement by the sensor but is an estimated range from multiple measurements. This is analogous to what is sometimes described as ‘modelled accuracy’ for commercial terrestrial laser scanners systems.

We obtain reference values for the distances with a reference instrument, a Leica RTC360 terrestrial laser scanner. The reference scan contains both the observed plane and the Livox scanner housing. We select a centre point on the sensor’s front face as the sensor’s origin from which the reference distance is calculated. The treatment of the point cloud on the plane is the same as for the investigated sensor unit.

The measurement is repeated 5 times at each distance, except for the furthest station where only 4 measurements were obtained. We do this to check repeatability of the range measurements. As a plane is fit to the point cloud, we can also calculate planarity as a RMS of the point cloud at each station.

The analysis of the range measurements is not conclusive. On the one hand analysis shows deviations are in the range of  $\pm 25$  millimetre. Larger deviations seem to occur primarily at longer distances. This is supported by observing that the standard

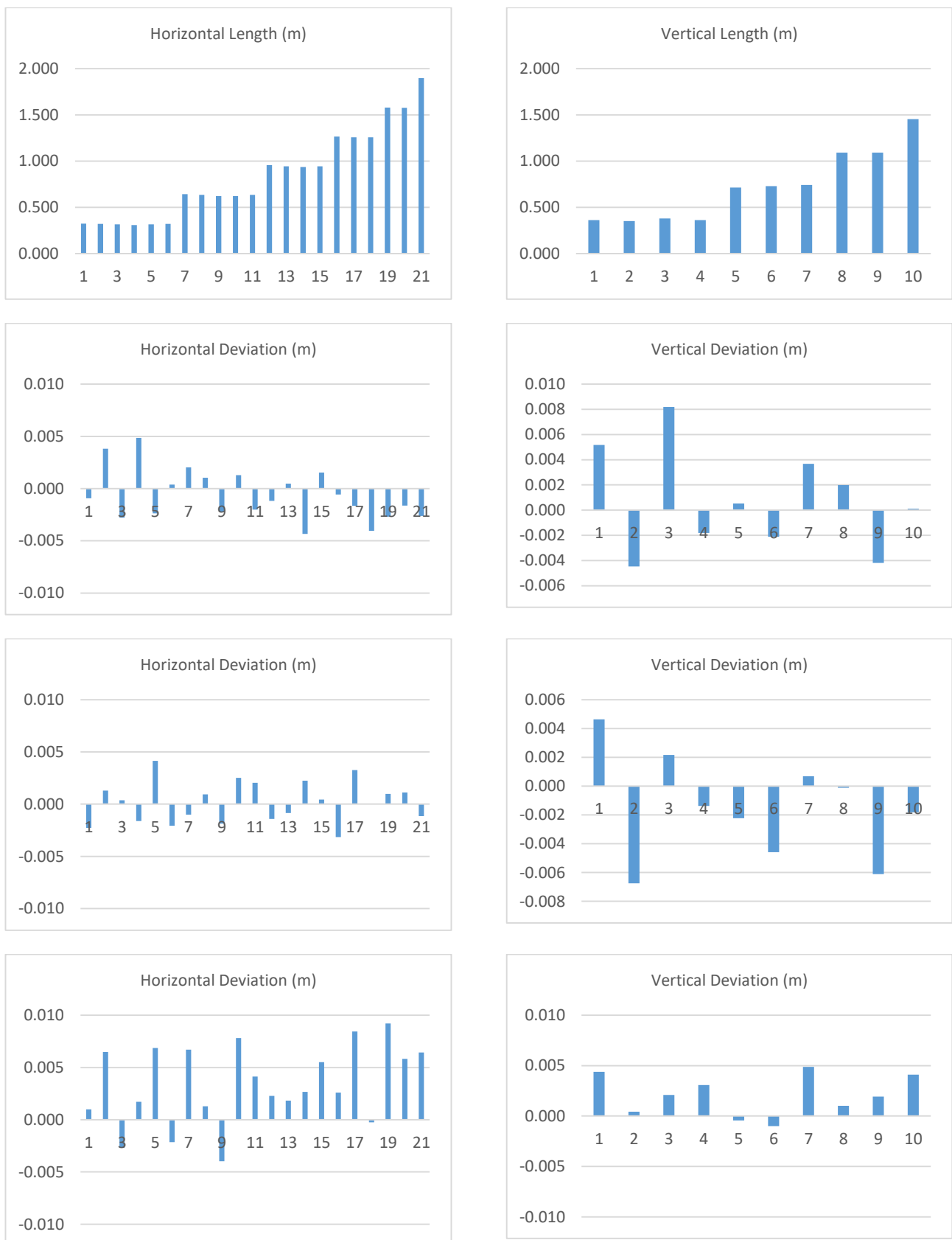


Figure 11: Length measurement experiments separated into horizontal length (first column) and vertical length (second column). The first row shows the absolute length measured. The following rows show deviations to the reference instrument at time interval 0, 5 and 30 minutes.

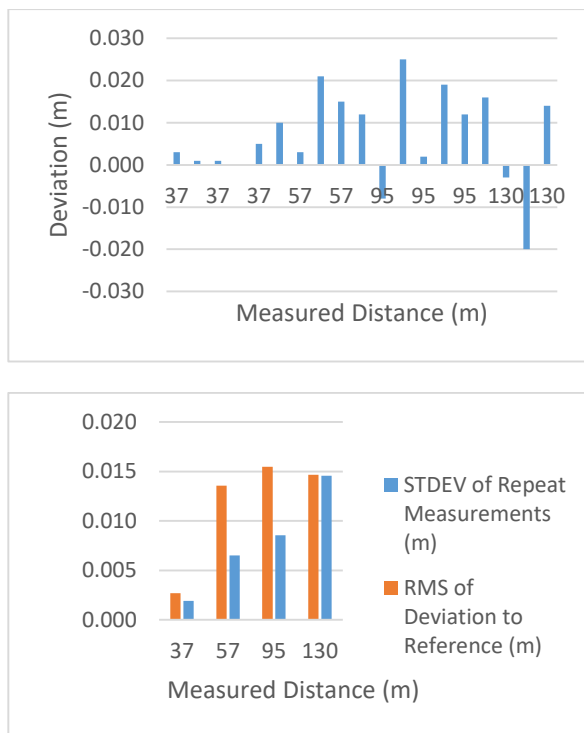


Figure 12: Deviations and repeatability for range measurements over longer distances.

deviation for the repeat measurements increases proportionally to the range. Contrary to this the RMS of the deviation to the reference for repeated measurements seems similar for all distances above 50 meters, but significantly smaller at 40 meters. so no clear dependency on distance can be found.

### 3.3 Flatness

The noise level of a sensor can often be assessed by checking the flatness of a point cloud over a reference plane. Obviously, at larger measurement volumes no certified test body for flatness exists. We therefore check flatness over the sand-stone façade of a building assumed to be flat. We check this with a reference instrument Leica RTC 360. The reference provides a plane fit with a standard deviation of 2 millimetres, with a maximum deviation of 5 millimetres. This is slightly worse than the instrument’s specification of 1 millimetre + 10 ppm range accuracy. However, it confirms the object’s flatness for the purpose of this experiment. We calculate the standard deviation of a plane-fit at the same distances as discussed above for each of the repeat measurements of the investigated sensor. Figure 13

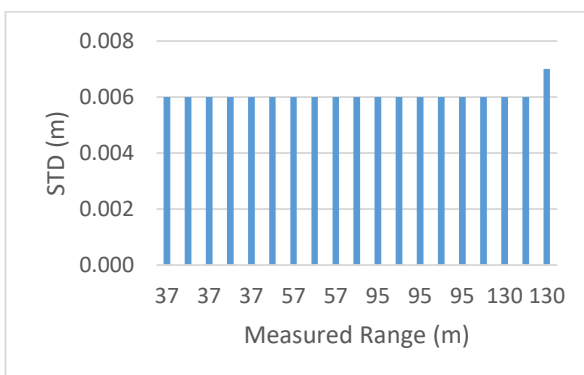


Figure 13: Plane fit quality over different ranges expressed as standard deviation of a plane fit.

shows the results obtained. The standard deviation is typically 6 millimetres. There is no visible dependency of flatness on the range.

## 4. CONCLUSIONS

The investigations have shown the capabilities of this very low-cost automotive LIDAR sensor. We can quantitatively characterize the sensors accuracy via the length measurement and range measurement tests. The sensor shows deviations in length measurement with a span of about 10 millimetres over short distances. This corresponds to an angular uncertainty of a tenth of a degree in the chosen setup. For close-range measurement this is clearly not a performance that would challenge existing surveying instruments. However, it is clearly within the range of specialized consumer-grade close-range sensors as described in (Boehm, 2014).

The standout feature of this sensor is its long-range capability which the manufacturer states as a maximum range of 260 meters. Our experiments show that at longer ranges the sensor unit achieves modelled distance measurements to an accuracy of  $\pm 20$  millimetres. The flatness over the tested distances is constant at a standard deviation of 6 millimetres. Again, this hardly challenges established survey instruments. However, there is a clear improvement over previous generations of automotive LIDAR systems as described in (Glennie and Lichti, 2011) and (Glennie et al., 2016). In addition, in our experiments we could not observe a degradation of measurements of the time span of  $\frac{1}{2}$  hour.

A remaining uncertainty in our set of experiments rests with the fact that the unusual scan pattern of the sensor has not allowed us to use standard commercial software to automatically measure target centroids. Instead they had to be measured manually, which introduces additional uncertainty. With the uneven point distribution, it is impossible to estimate point density in the target areas. Visual assessment shows that point spacing around the target centres is in the order of a few millimetres. Therefore, manual target measurement clearly is a limiting factor in the length measurement experiments.

Further issues with the sensor that had an effect on the testing procedure could not be characterised quantitatively. They include the radiometric influences on range measurements. This is clearly an unwanted effect that again limits point-wise measurement accuracy. There also seems to be a systematic influence of the deflection angle which manifests itself in concentric ripples on a planar surface. This is most prominently visible at close-range. On longer ranges the general noise in the point cloud seems to hide this effect.

Within the work described here we have made no attempt to correct or calibrate for any of the effects described. At the moment there is not enough experience with the sensor to attempt this. Future work should concentrate on automating target measurement or identifying more suitable targets. This would increase confidence in the obtained values and potentially uncover further systematic patterns in the sensor’s performance.

## ACKNOWLEDGEMENTS

Some of the work described in this publication was carried out as part of A. Ortiz Arteaga’s research project in fulfilment of the MSc degree in Geospatial Sciences at University College London.

## REFERENCES

- Boehm, J., 2014. Accuracy Investigation for Structured-light Based Consumer 3D Sensors. *Photogramm. - Fernerkund. - Geoinformation* 2014, 117–127. <https://doi.org/10.1127/1432-8364/2014/0214>
- Girardeau-Montaut, D., 2011. CloudCompare-Open Source project. OpenSource Proj.
- Glennie, C., Lichti, D.D., 2011. Temporal Stability of the Velodyne HDL-64E S2 Scanner for High Accuracy Scanning Applications. *Remote Sens.* 3, 539–553. <https://doi.org/10.3390/rs3030539>
- Glennie, C.L., Kusari, A., Facchin, A., 2016. Calibration and Stability Analysis of the VLP-16 Laser Scanner. *ISPRS-Int. Arch. Photogramm. Remote Sens. Spat. Inf. Sci.* 55–60.
- LAS Specification Version 1.3, 2009.
- Ling, Z., Yuqing, M., Ruoming, S., 2008. Study on the Resolution of Laser Scanning Point Cloud, in: *IGARSS 2008 - 2008 IEEE International Geoscience and Remote Sensing Symposium*. IEEE, Boston, MA, USA, pp. II-1136-II-1139. <https://doi.org/10.1109/IGARSS.2008.4779200>
- Livox, 2019a. Livox Mid Series User Manual v1.2.
- Livox, 2019b. Livox Viewer 0.5.0 [WWW Document]. URL <https://www.livoxtech.com/hub/downloads>
- Livox Technology, 2019. Mid-40 lidar sensor - Livox [WWW Document]. URL <https://www.livoxtech.com/mid-40-and-mid-100> (accessed 10.30.19).
- Marshall, G.F., 1999. Risley prism scan patterns, in: Beiser, L., Sagan, S.F., Marshall, G.F. (Eds.), . Presented at the SPIE's International Symposium on Optical Science, Engineering, and Instrumentation, Denver, CO, pp. 74–86. <https://doi.org/10.1117/12.351658>
- Moras, J., Rodriguez, F.S.A., Drevelle, V., Dherbomez, G., Cherfaoui, V., Bonnifait, P., 2012. Drivable space characterization using automotive lidar and georeferenced map information, in: *2012 IEEE Intelligent Vehicles Symposium*. Presented at the 2012 IEEE Intelligent Vehicles Symposium (IV), IEEE, Alcal de Henares , Madrid, Spain, pp. 778–783. <https://doi.org/10.1109/IVS.2012.6232252>
- Royal Institution of Chartered Surveyors, 2014. Measured surveys of land, buildings and utilities: RICS guidance note, global.
- Thomson, C., Boehm, J., 2014. Indoor Modelling Benchmark for 3D Geometry Extraction. *ISPRS - Int. Arch. Photogramm. Remote Sens. Spat. Inf. Sci.* XL-5, 581–587. <https://doi.org/10.5194/isprsarchives-XL-5-581-2014>
- THORLABS, 2019. Risley Prism Scanner [WWW Document]. URL [https://www.thorlabs.com/images/tabimages/Risley\\_Prism\\_Scanner\\_App\\_Note.pdf](https://www.thorlabs.com/images/tabimages/Risley_Prism_Scanner_App_Note.pdf)
- VDI-Richtlinie: VDI/VDE 2634 Blatt 2 - Optische 3D-Messsysteme - Bildgebende Systeme mit flächenhafter Antastung, 2002.